

First-Principle Predictions of Electronic Properties and Half-Metallic Ferromagnetism in Vanadium-Doped Rock-Salt SrO

MOHAMED BERBER,^{1,7} BENDOUMA DOUMI ,^{2,8}
ALLEL MOKADDEM,^{1,3,9} YESIM MOGULKOC,⁴ ADLANE SAYEDE,⁵
and ABDELKADER TADJER⁶

1.—Centre Universitaire Nour Bachir El Bayadh, 32000 El Bayadh, Algeria. 2.—Faculty of Sciences, Department of Physics, Dr. Tahar Moulay University of Saida, 20000 Saida, Algeria. 3.—Theoretical Physics Laboratory, U.S.T.H.B. Algiers, Bab Ezzouar, Algeria. 4.—Department of Engineering Physics, Faculty of Engineering, Ankara University, 06100 Tandogan, Ankara, Turkey. 5.—Unité de Catalyse et Chimie du Solide (UCCS), UMR CNRS 8181, Faculté des Sciences, Université d'Artois, Rue Jean Souvraz, SP 18, 62307 Lens, France. 6.—Modelling and Simulation in Materials Science Laboratory, Physics Department, Djillali Liabes University of Sidi Bel-Abbes, 22000 Sidi Bel Abbès, Algeria. 7.—e-mail: berbermohamed@yahoo.fr. 8.—e-mail: bdoumami@yahoo.fr. 9.—e-mail: mokaddem.allel@gmail.com

We have used first-principle methods of density functional theory within the full potential linearized augmented plane wave scheme to investigate the electronic and magnetic properties of cubic rock-salt, SrO, doped with vanadium (V) impurity as $\text{Sr}_{1-x}\text{V}_x\text{O}$ at various concentrations, $x = 0.25, 0.5,$ and 0.75 . We have found that the ferromagnetic state arrangement of $\text{Sr}_{1-x}\text{V}_x\text{O}$ is more stable compared to the anti-ferromagnetic state configuration. The electronic structures have a half-metallic (HM) ferromagnetic (F) behavior for $\text{Sr}_{0.75}\text{V}_{0.25}\text{O}$ and $\text{Sr}_{0.5}\text{V}_{0.5}\text{O}$. This feature results from the metallic and semi-conducting natures of majority-spin and minority-spin bands, respectively. The HMF gap decreases with the increasing concentration of vanadium atoms due to the broadening of $3d$ (V) levels in the gap, and hence the $\text{Sr}_{0.25}\text{V}_{0.75}\text{O}$ becomes metallic ferromagnetic. The $\text{Sr}_{0.75}\text{V}_{0.25}\text{O}$ revealed a large HM gap with spin polarization of 100%. The $\text{Sr}_{1-x}\text{V}_x\text{O}$ compound at low concentrations seems a better candidate to explore the half-metallicity for practical spintronics applications.

Key words: Electronic structures, magnetic properties, half-metallic gap, ferromagnetic arrangement

INTRODUCTION

Spintronics (spin electronics)¹ is a recent discipline of electronics that exploits the concept of electron spin (spin magnetic moment) as a new degree of freedom of an electron in addition to its charge, for information processing and storage.^{1,2} The expected advantage of spintronic devices with respect to the conventional electronic ones would be

nonvolatility, increased data processing speed, increased transistor density and decreased power consumption.³ The dilute magnetic semiconductors (DMSs)-based III–V and II–VI-type-semiconductors are the main candidates for the development of spintronics applications technology, as they exhibit a half-metallic character^{4,5} and their ferromagnetic state is stable at temperatures higher than room temperature.^{6,7}

Rock-salt strontium oxide (SrO) belongs to the II–VI alkaline-earth chalcogenides, which are very important semiconductors with large band gaps and valence band widths.⁸ SrO has attracted increasing

(Received March 31, 2017; accepted September 7, 2017; published online September 19, 2017)

interest because of its applications in various technologies ranging from catalysis to microelectronics.⁹ SrO has the rock-salt crystal structure with a lattice constant of 5.16 Å and a nonmagnetic band insulator with a forbidden gap of 5.3 eV.¹⁰ According to the theoretical and experimental results of substituted oxygen by nitrogen in SrO, this compound is considered as a potential candidate as a DMS.¹⁰ Also, Pardo and al.¹¹ have predicted the induced magnetism in SrO by the effect of substituted N impurities at O sites, using the local density approximation of adding an empirical Hubbard (U) potential (LDA + U) developed by Anisimov et al.^{12,13} The materials include 3d states and have wide gaps with experimental studies and LDA + U. In the LDA + U method,^{12,13} the effective on-site interactions are introduced to the existing Hamiltonian to better account for the orbital dependence of the Coulomb and exchange interactions of the strongly correlated *d* and *f* electrons.¹⁴ This approach can significantly improve the band gaps and magnetic moments for magnetically ordered states.¹⁵ Recently, the electronic and magnetic properties have been predicted in strontium SrX (X = S, Se and Te) chalcogenide semiconductors doped with transition chromium¹⁶ and vanadium atoms.¹⁷ Also, Berri et al.¹⁸ have predicted the half-metallic ferromagnetism in the Sr_{1-x}Cr_xO and Sr_{1-x}Mn_xO compounds at concentrations *x* = 0.25 and 0.75 of Cr and Mn atoms.

In this study, we have determined the structural, electronic and magnetic properties of SrO doped with transition metal vanadium (V) atoms as Sr_{1-x}V_xO compounds at various concentrations of *x* = 0.25, 0.5, and 0.75. We have predicted the structural parameters, the spin-polarized band structures and the densities of states, magnetic moments and the half-metallic behavior of the doped systems by using first-principle methods of the linearized augmented plane wave scheme with the generalized gradient approximation proposed in 2006 by Wu and Cohen (GGA-WC).¹⁹

METHOD OF CALCULATIONS

We have calculated the structural, electronic and magnetic properties of Sr_{1-x}V_xO compounds at different concentrations of *x* = 0.25, 0.5, and 0.75 of vanadium (V) impurities. The calculations have been performed by the use of first-principles methods of density functional theory^{20,21} within the WIEN2k package,²² based on the full potential linearized augmented plane wave (FP-LAPW) approach, where the exchange and correlation potential is treated by GGA-WC.⁹ The charge density was Fourier-expanded up to $G_{\max} = 14$ (a.u.)⁻¹, where G_{\max} is the largest vector in the Fourier expansion, while the basic functions and potential are extended in combination with spherical harmonics around the atomic sites with a cutoff of $l_{\max} = 10$ of atomic spheres. The Fourier series in the

interstitial region are extended in plane waves with a cutoff of $R_{\text{MT}} K_{\max} = 9.5$ (where R_{MT} is the mean radius of Muffin-tin spheres). We have used the 666 k-points of the Monkhorst–Pack mesh^{23,24} in the sampling of the Brillouin zone. The self-consistent convergence of the total energy was set at 0.1 mRy.

RESULTS AND DISCUSSION

Magnetic Stability, Formation Energies and Structural Parameters

SrO is a binary II–VI semiconductor type that crystallizes in the rock-salt NaCl (B1) structure with the space group of $Fm\bar{3}m$ No. 225, where the Sr and O atoms are situated, respectively, at the (0, 0, 0) and (0.5, 0.5, 0.5) positions. The Sr₃VO₄, Sr₂V₂O₄ and SrV₃O₄ supercells of 8 atoms are obtained, respectively, by the substitution of one, two and three Sr atoms by vanadium (V) impurities. We obtained Sr_{0.75}V_{0.25}O, Sr_{0.5}V_{0.5}O and Sr_{0.25}V_{0.75}O for concentrations of *x* = 0.25, 0.5, and 0.75, respectively. The Sr_{0.75}V_{0.25}O and Sr_{0.25}V_{0.75}O have cubic structures with the space group of $Pm\bar{3}m$ No. 221, and the Sr_{0.5}Cr_{0.5}O has a tetragonal structure with the space group of $P4/mmm$ No. 123 (see Fig. 1).

To determine the magnetic stability in the ferromagnetic (FM) or anti-ferromagnetic (AFM) state configurations, we have computed the energy differences $\Delta E = E_{\text{AFM}} - E_{\text{FM}}$ between the total energies of the FM and AFM states of Sr_{1-x}V_xO compounds at various concentrations. We have found that the total energy differences are 0.087 eV, 0.124 eV, and 3.96 eV for Sr_{0.75}V_{0.25}O, Sr_{0.5}V_{0.5}O and Sr_{0.25}V_{0.75}O, respectively. Therefore, the positive values of ΔE suggest that these compounds are more stable in the ferromagnetic state configuration than in the anti-ferromagnetic state.

The phase stability in the solid states is measured by the formation energy.^{25,26} To verify the phase stability of the Sr_{0.75}V_{0.25}O, Sr_{0.5}V_{0.5}O and Sr_{0.25}V_{0.75}O supercells, we have calculated the formation energies by using the following expression^{27,28}:

$$E_{\text{form}} = E_{\text{total}}(\text{Sr}_{4-y}\text{V}_y\text{O}_4) - \frac{(4-y)E_{\text{tot}}^0(\text{Sr})}{8} - \frac{yE_{\text{tot}}^0(\text{V})}{8} - \frac{4E_{\text{tot}}^0(\text{O})}{8} \quad (1)$$

where the $E_{\text{total}}(\text{Sr}_{4-y}\text{V}_y\text{O}_4)$ is the total energy per atom of Sr_{4-y}V_yO₄, and the *y* is the number of substitute V atoms in the supercell, equal to 1, 2, and 3 for concentrations *x* = 0.25, 0.5, and 0.75, respectively. The $E_{\text{tot}}^0(\text{Sr})$, $E_{\text{tot}}^0(\text{V})$ and $E_{\text{tot}}^0(\text{O})$ are the total energies per atom of Sr, V and O bulk, respectively. The formation energies are -3.04, -2.59, -2.22 eV for Sr_{0.75}V_{0.25}O, Sr_{0.5}V_{0.5}O and Sr_{0.25}V_{0.75}O, respectively. Consequently, the negative values of the formation energies mean that our compounds are thermodynamically stable in the ferromagnetic rock-salt phase.

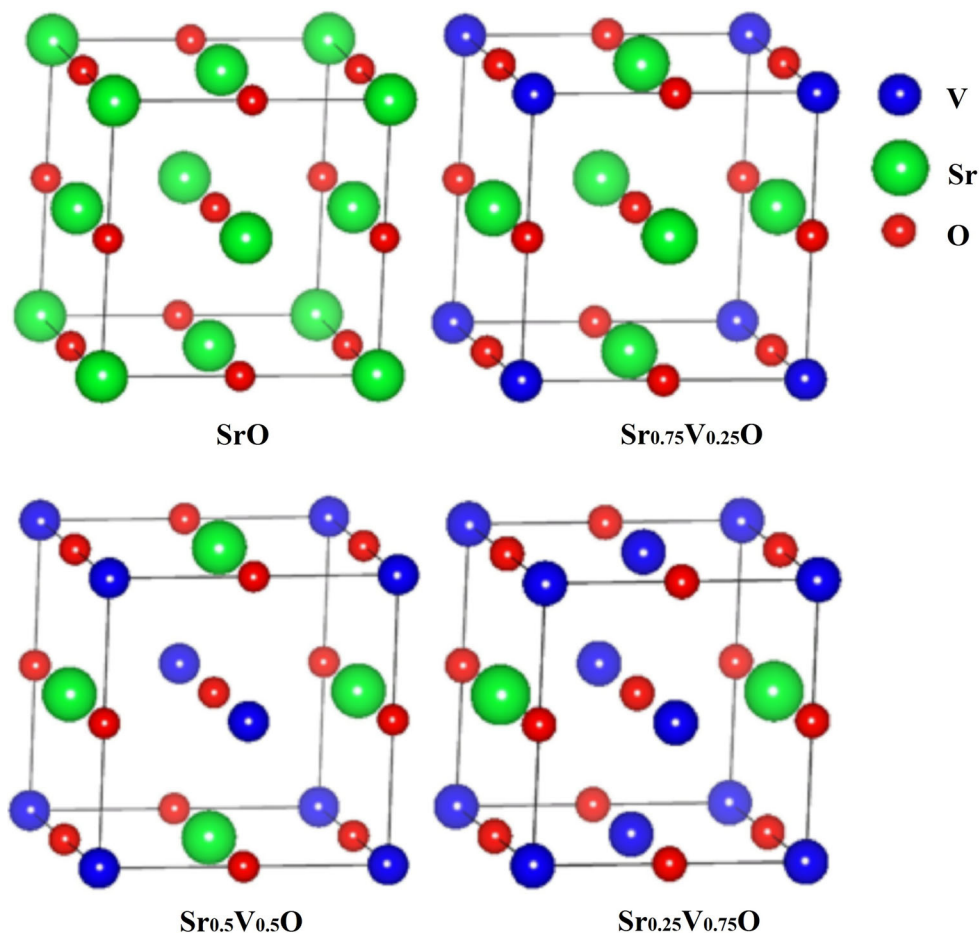

 Fig. 1. Crystal structures of SrO, Sr_{0.75}V_{0.25}O, Sr_{0.5}V_{0.5}O and Sr_{0.25}V_{0.75}O.

Table I. Calculated lattice constant (a), bulk modulus (B) and its pressure derivative (B') for SrO and Sr_{1-x}V_xO at concentrations of $x = 0.25, 0.5$, and 0.75 of V atoms

| Compound | Method | Concentration (x) | a (Å) | B (GPa) | B' |
|--|--------------|-----------------------|-----------------------|---------------------|--------------------|
| This work | | | | | |
| SrO | GGA-WC | 0 | 5.127 | 92.04 | 4.46 |
| Sr _{0.75} V _{0.25} O | | 0.25 | 4.980 | 107.36 | 4.43 |
| Sr _{0.5} V _{0.5} O | | 0.5 | 4.762 | 119.46 | 4.12 |
| Sr _{0.25} V _{0.75} O | | 0.75 | 4.535 | 124.23 | 3.80 |
| Other calculations | | | | | |
| SrO | GGA-WC | 0 | 5.21 ¹⁸ | 83.04 ¹⁸ | 4.21 ¹⁸ |
| | Experimental | | 5.16 ^{30,31} | 91 ³¹ | 4.3 ³¹ |

To calculate the structural properties of binary SrO and ferromagnetic Sr_{1-x}V_xO ternary compounds at different concentrations x , we have fitted the variation of the total energies as a function of volumes with the Murnaghan equation.²⁹ The obtained structural parameters, such as lattice constants (a), bulk modulus (B) and their pressure derivatives (B') of SrO and Sr_{1-x}V_xO with theoretical¹⁸ and experimental data,^{30,31} are given in Table I, which shows that our results of the a , B

and B' parameters of SrO maintain good agreement with the theoretical calculations¹⁸ found by the same GGA-WC approach,¹⁹ and stay close to the experimental ones.^{30,31}

We have noticed that the lattice parameter of SrO is higher than that of Sr_{1-x}V_xO compounds, indicating that the vanadium (V) ionic radius is smaller than that of Sr. This implies that the bulk modulus of Sr_{1-x}V_xO-doped materials are higher than that of SrO. Therefore, the binary SrO is more easily

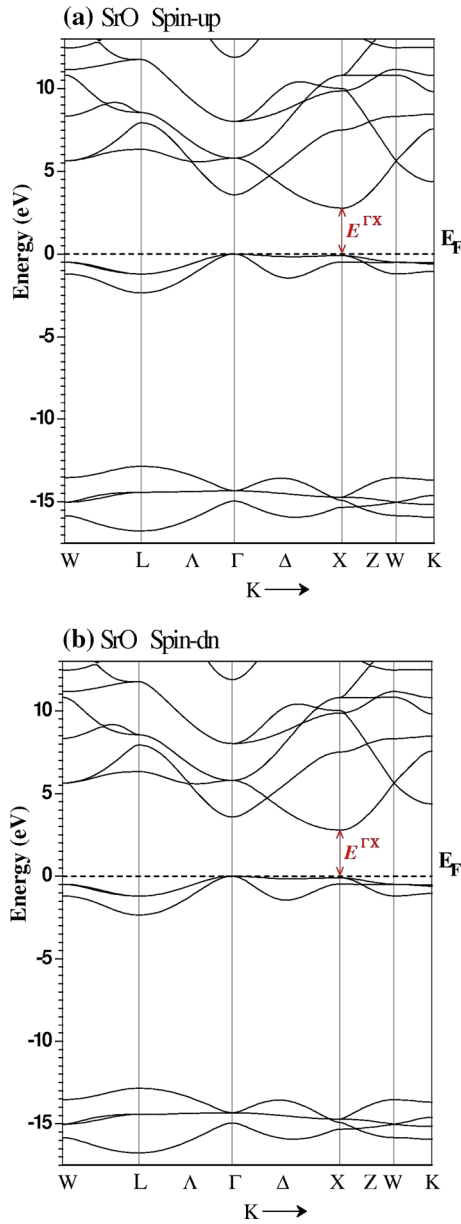


Fig. 2. Spin-polarized band structures for SrO. (a) Majority spin (up) and (b) minority spin (dn). The Fermi level is set to zero (horizontal dotted line).

compressible than $\text{Sr}_{1-x}\text{V}_x\text{O}$ -doped systems. In the following section, the optimized lattice constants were used to calculate the electronic and magnetic properties of SrO and $\text{Sr}_{1-x}\text{V}_x\text{O}$ compounds.

Electronic Structures with Half-Metallic Behavior

Figures 2, 3, 4, and 5 display the computed spin-polarized band structures at high symmetry points in the Brillouin zone of SrO, $\text{Sr}_{0.75}\text{V}_{0.25}\text{O}$, $\text{Sr}_{0.5}\text{V}_{0.5}\text{O}$ and $\text{Sr}_{0.25}\text{V}_{0.75}\text{O}$, respectively. Figure 2, of SrO, reveals similar band structures for both majority

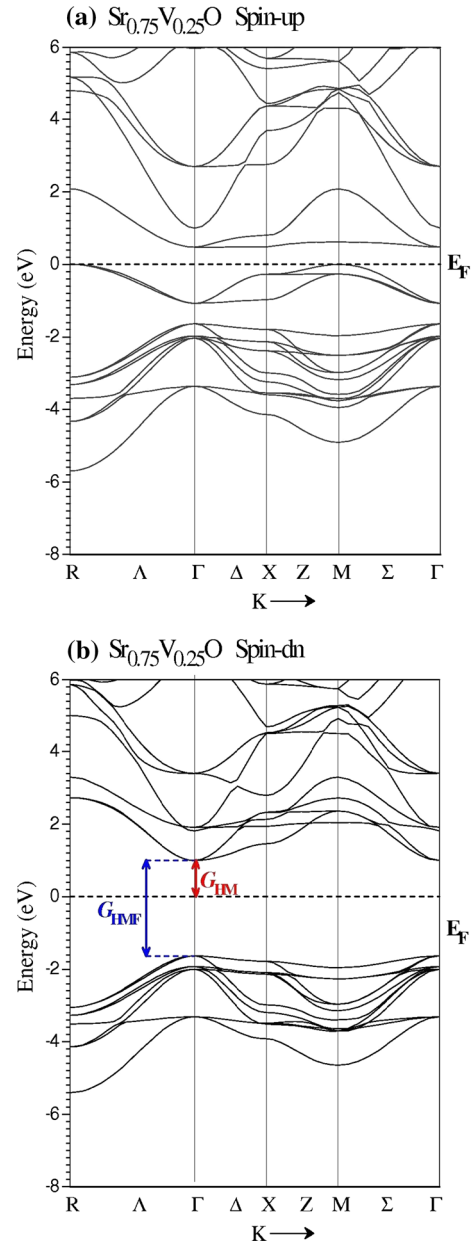


Fig. 3. Spin-polarized band structures for $\text{Sr}_{0.75}\text{V}_{0.25}\text{O}$. (a) Majority spin (up) and (b) minority spin (dn). The Fermi level is set to zero (horizontal dotted line).

and minority spin, which are characterized by a semiconductor character with an indirect band gap ($E^{\Gamma X}$) located between Γ and X high-symmetry points. In distinguishing the band structures of $\text{Sr}_{1-x}\text{V}_x\text{O}$ at concentrations of $x = 0.25$ and 0.5 , Figs. 3 and 4 show that the majority-spin bands are metallic whereas a gap occurs at the Fermi level for the minority-spin bands. As a result, the $\text{Sr}_{1-x}\text{V}_x\text{O}$ -doped systems at $x = 0.25$, and 0.5 behave a half-metallic ferromagnetic feature with 100% spin polarization around the Fermi level. We have noticed that the conduction band minimum shifted

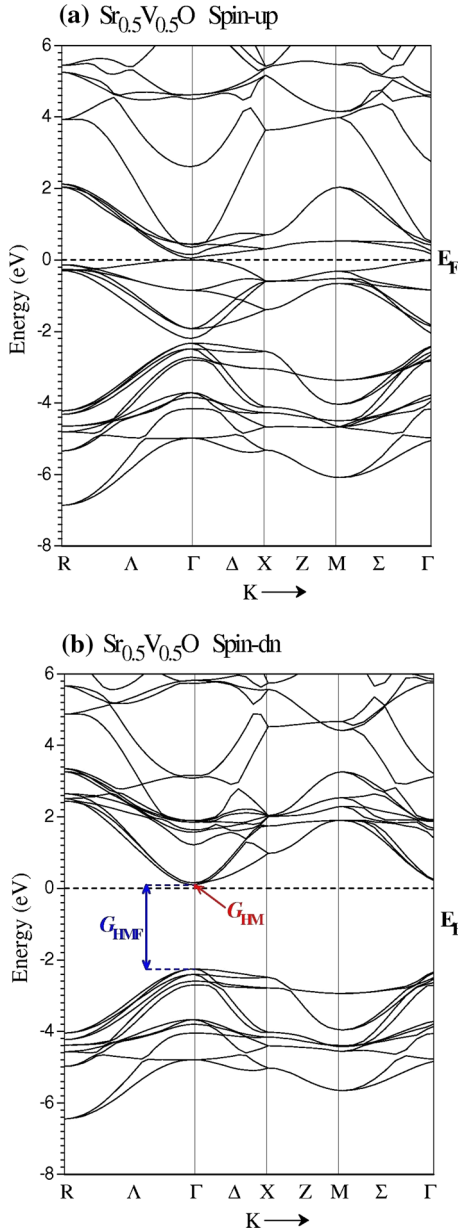


Fig. 4. Spin-polarized band structures for $\text{Sr}_{0.5}\text{V}_{0.5}\text{O}$. (a) Majority spin (up) and (b) Minority spin (dn). The Fermi level is set to zero (horizontal dotted line).

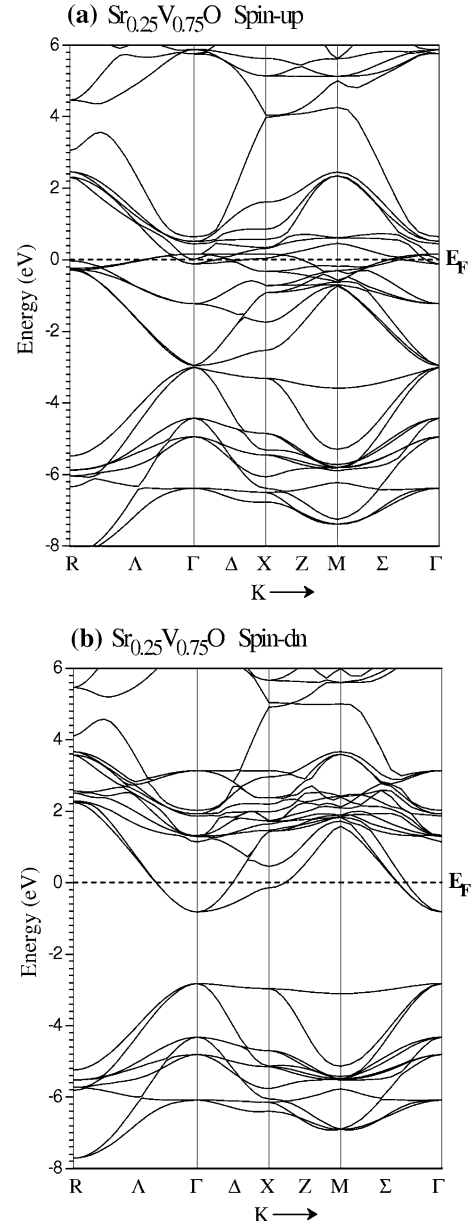


Fig. 5. Spin-polarized band structures for $\text{Sr}_{0.25}\text{V}_{0.75}\text{O}$. (a) Majority spin (up) and (b) Minority spin (dn). The Fermi level is set to zero (horizontal dotted line).

towards the Fermi level due to the broadening of $3d$ (V) states in the gap, and hence the $\text{Sr}_{0.25}\text{V}_{0.75}\text{O}$ becomes metallic ferromagnetic (see Fig. 5).

For $\text{Sr}_{0.75}\text{V}_{0.25}\text{O}$ and $\text{Sr}_{0.5}\text{V}_{0.5}\text{O}$, the half-metal (HM) ferromagnetic (F) gap (G_{HMF}) and HM gap (G_{H}) are generated in the minority-spin bands due to the large p - d exchange coupling between the $3d$ (V) and p (O) levels. G_{HMF} describes a direct band gap at Γ high-symmetry point that separates the valence band maximum (VBM) and the conduction band minimum (CBM). Nevertheless, the HM (spin-flip) gap is defined to be the minimum energy with respect to the Fermi level of the majority (minority) spin between the lowest energy of the conduction

bands and the absolute value of highest energy of the valence bands.^{32,33} In our case, the HM gap determines the minimal energy situated between the Fermi level and CBM for $\text{Sr}_{0.75}\text{V}_{0.25}\text{O}$ and $\text{Sr}_{0.5}\text{V}_{0.5}\text{O}$. The results of the indirect band gap ($E^{\Gamma X}$) of SrO, G_{HMF} and G_{H} of the minority-spin bands of $\text{Sr}_{0.75}\text{V}_{0.25}\text{O}$ and $\text{Sr}_{0.5}\text{V}_{0.5}\text{O}$ with other theoretical³⁴ and experimental data³⁵ are given in Table II, which shows that the $E^{\Gamma X}$ indirect gap of SrO is in good agreement with the theoretical result of Labidi et al.³⁴ calculated by the generalized gradient approximation of Perdew et al. (GGA-PBE).³⁶ Figures 3 and 4 show a direct HMF gap, which decreases from $\text{Sr}_{0.75}\text{V}_{0.25}\text{O}$ to $\text{Sr}_{0.5}\text{V}_{0.5}\text{O}$ due

Table II. Calculated indirect band gap E^{IX} for SrO, half-metallic ferromagnetic gap (G_{HMF}) and half-metallic gap (G_{HM}) of minority-spin band for $\text{Sr}_{1-x}\text{V}_x\text{O}$ at concentrations $x = 0.25$ and 0.5 of V atoms

| Compound | Method | Concentration (x) | G_{HMF} (eV) | G_{HM} (eV) | E^{IX} (eV) | Behavior |
|---|--------------|-----------------------|-----------------------|----------------------|----------------------|----------|
| This work | | | | | | |
| SrO | GGA-WC | 0 | | | 2.782 | |
| $\text{Sr}_{0.75}\text{V}_{0.25}\text{O}$ | | 0.25 | 2.634 | 1.00 | | HMF |
| $\text{Sr}_{0.5}\text{V}_{0.5}\text{O}$ | | 0.5 | 2.359 | 0.10 | | HMF |
| $\text{Sr}_{0.25}\text{V}_{0.75}\text{O}$ | | 0.75 | | | | MF |
| Other calculations | | | | | | |
| SrO | GGA-PBE | 0 | | | 3.335 ³⁴ | |
| | Experimental | | | | 5.71 ³⁵ | |

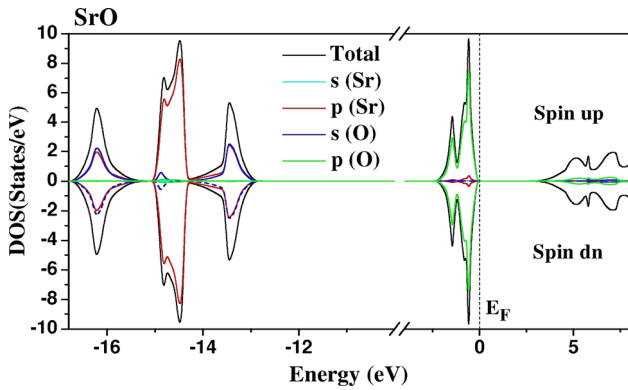


Fig. 6. Spin-polarized total and partial densities of states of SrO. The Fermi level is set to zero (vertical dotted line).

to the broadening of the $3d$ (V) states in the gap. In addition, the $\text{Sr}_{0.75}\text{V}_{0.25}\text{O}$ revealed a higher HM gap of 1.0 eV, and hence the $\text{Sr}_{1-x}\text{V}_x\text{O}$ at a low concentration of vanadium impurity seems to be potential material for future spintronics applications.

Moreover, to investigate the origin of the ferromagnetic arrangement in $\text{Sr}_{1-x}\text{V}_x\text{O}$, we have computed the total (T) and partial (P) densities of states (DOS) of $\text{Sr}_{1-x}\text{V}_x\text{O}$ at different concentrations. The spin-polarized TDOS and PDOS of SrO, $\text{Sr}_{0.75}\text{V}_{0.25}\text{O}$, $\text{Sr}_{0.5}\text{V}_{0.5}\text{O}$ and $\text{Sr}_{0.25}\text{V}_{0.75}\text{O}$ are presented in Figs. 6, 7, 8, and 9, respectively. Figure 6, of SrO, shows symmetrical states between the spin-up and spin-down directions with a semiconductor feature, confirming the non-magnetic nature of this compound. The valence bands of SrO in the ranges -15 eV to -14 eV and -2.5 eV to 0 eV are principally formed by the p (Sr) and p (O) states, respectively. The TDOS of $\text{Sr}_{1-x}\text{V}_x\text{O}$ -doped systems depicted non-symmetrical states of spin-up and spin-down due to strong p - d hybridization between the p (O) and $3d$ (V) states around the Fermi level for the majority-spin direction. This hybridization occurs mainly at the top of the majority-spin valence bands and crosses the Fermi level, leading to the metallic nature for all $\text{Sr}_{1-x}\text{V}_x\text{O}$ compounds. On the

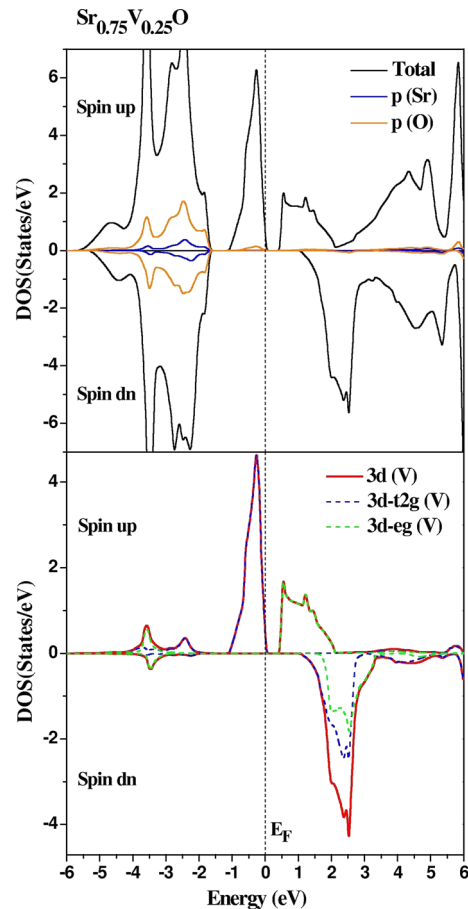


Fig. 7. Spin-polarized total and partial densities of states of $\text{Sr}_{0.75}\text{V}_{0.25}\text{O}$. The Fermi level is set to zero (vertical dotted line).

other hand, the minority-spin states for the concentrations $x = 0.25$, and 0.5 show a gap around the Fermi level. Therefore, the $\text{Sr}_{0.75}\text{V}_{0.25}\text{O}$ and $\text{Sr}_{0.5}\text{V}_{0.5}\text{O}$ materials are half-metallic ferromagnets with spin polarization of 100%.

In the octahedrally $\text{Sr}_{1-x}\text{V}_x\text{O}$ structures, the vanadium (V) atom is surrounded by six oxygen (O) ions which create an octahedral crystal field.

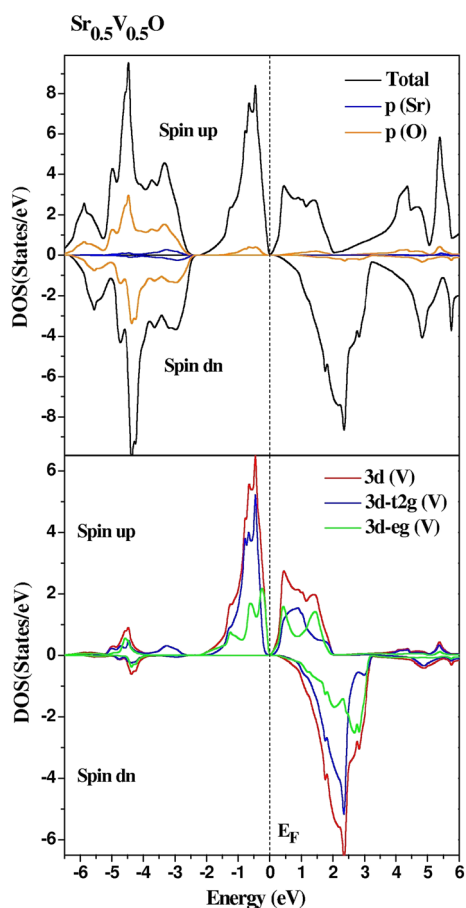


Fig. 8. Spin-polarized total and partial densities of states of $\text{Sr}_{0.5}\text{V}_{0.5}\text{O}$. The Fermi level is set to zero (vertical dotted line).

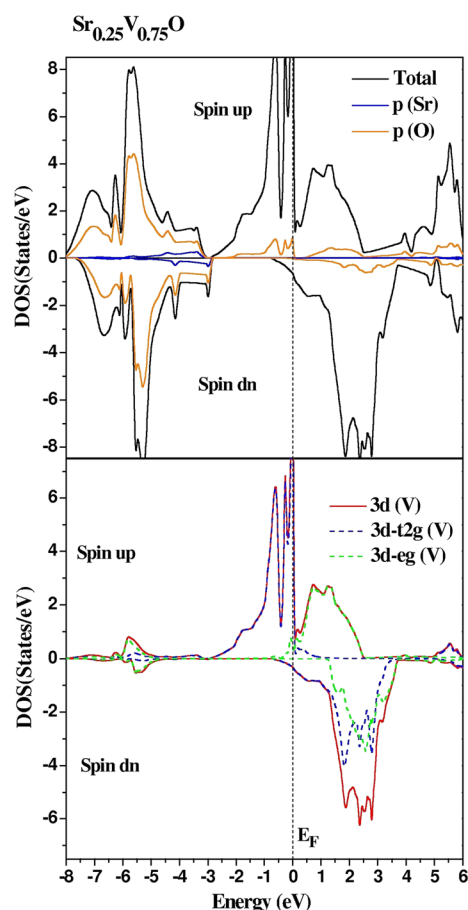


Fig. 9. Spin-polarized total and partial densities of states of $\text{Sr}_{0.25}\text{V}_{0.75}\text{O}$. The Fermi level is set to zero (vertical dotted line).

Figure 7 shows that the octahedral crystal field splits the 3d (V) orbitals into three low-lying t_{2g} (d_{xy}, d_{xz}, d_{yz}) states and two high-lying e_g (d_{z^2} and $d_{x^2-y^2}$) symmetry states.^{16,17} Sato et al.^{6,37} predicted the ferromagnetic state in magnetic semiconductors by the partially occupied anti-bonding states related to the double exchange mechanism. In the $\text{Sr}_{1-x}\text{V}_x\text{O}$ doped systems, the ferromagnetic state arrangement is stabilized by the large hybridization between the p (O) and the partially occupied 3d (V) levels associated with double exchange mechanism.³⁸

Magnetic Properties

In the $\text{Sr}_{1-x}\text{V}_x\text{O}$ doped systems, the localized 3 (d) states of the V atom contribute two electrons to delocalized carriers of the valence bands, and thus the 3 (d) majority-spin states of the V ion become partially filled with three electrons. These impaired electrons create a total magnetic moment of $3 \mu_B$ (μ_B is the Bohr magneton) per vanadium atom. The calculated total and partial magnetic moments of V, Sr and O per V atom and in the interstitial sites of $\text{Sr}_{0.75}\text{V}_{0.25}\text{O}$, $\text{Sr}_{0.5}\text{V}_{0.5}\text{O}$ and $\text{Sr}_{0.25}\text{V}_{0.75}\text{O}$ are summarized in Table III, which shows that the total

magnetic moments are principally formed by the contribution of the V atoms. Owing to the p - d exchange interaction, the partial moments of the V atoms are reduced less than $3 \mu_B$ and smaller partial magnetic moments are induced at non-magnetic Sr and O sites. For $\text{Sr}_{0.75}\text{V}_{0.25}\text{O}$, the anti-ferromagnetic coupling is observed between the anti-parallel magnetic spins of V and O atoms, while the ferromagnetic interaction is revealed between the positive V and Sr magnetic spins. For both $\text{Sr}_{0.5}\text{V}_{0.5}\text{O}$ and $\text{Sr}_{0.25}\text{V}_{0.75}\text{O}$, the positive V, Sr and O magnetic moments suggest the ferromagnetic interaction between the V and (Sr, O) magnetic spins.

CONCLUSION

We have investigated the structural, electronic and magnetic properties of binary SrO and $\text{Sr}_{1-x}\text{V}_x\text{O}$ -doped compounds by the use of density functional theory within the full-potential linearized augmented-plane wave method with GGA-WC exchange and correlation potential. We have found that SrO is a semiconductor material, while $\text{Sr}_{0.75}\text{V}_{0.25}\text{O}$ and $\text{Sr}_{0.5}\text{V}_{0.5}\text{O}$ are half-metallic ferromagnetic. The $\text{Sr}_{0.75}\text{V}_{0.25}\text{O}$ shows a large HM gap with a spin polarization of 100%. The 3d (V) levels

Table III. Calculated total and local magnetic moments per V atom (in Bohr magneton μ_B) within the muffin-tin spheres and in the interstitial sites for $Sr_{1-x}V_xO$ at concentrations of $x = 0.25, 0.5$ and 0.75 of V atoms

| Compound | Concentration (x) | Total (μ_B) | V (μ_B) | Sr (μ_B) | O (μ_B) | Interstitial (μ_B) |
|----------------------|-----------------------|-------------------|---------------|----------------|---------------|--------------------------|
| $Sr_{0.75}V_{0.25}O$ | 0.25 | 3 | 2.483 | 0.013 | -0.0008 | 0.507 |
| $Sr_{0.5}V_{0.5}O$ | 0.5 | 3 | 2.436 | 0.008 | 0.025 | 0.534 |
| $Sr_{0.25}V_{0.75}O$ | 0.75 | 2.87 | 2.086 | 0.006 | 0.055 | 0.721 |

broaden strongly in the gap, leading to a metallic ferromagnetic nature for $Sr_{1-x}V_xO$ at the higher concentration of $x = 0.75$. The ferromagnetic state of $Sr_{1-x}V_xO$ is explained by the exchange coupling between p (O) and the partially filled $3d$ (V) states related to the double exchange mechanism. From our finding, the $Sr_{1-x}V_xO$ -doped compound at a low concentration of vanadium impurity is predicted to be a potential candidate for future spintronics applications.

REFERENCES

1. S.A. Wolf, D.D. Awschalom, R.A. Buhrman, J.M. Daughton, S. von Molnar, M.L. Roukes, A.V. Chitchekanova, and D.M. Treger, *Science* 294, 1488 (2001).
2. I. Žutić, J. Fabian, and S. Das Sarma, *Rev. Mod. Phys.* 76, 323 (2004).
3. M. Kaminska, A. Twardowski, and D. Wasik, *J. Mater. Sci. Mater. Electron.* 19, 828 (2008).
4. B. Doumi, A. Mokaddem, A. Sayede, F. Dahmane, Y. Mogulkoc, and A. Tadjer, *Superlattices Microstruct.* 88, 139 (2015).
5. B. Doumi, A. Mokaddem, A. Sayede, M. Boutaleb, A. Tadjer, F. Dahmane, and J. Supercond, *Nov. Magn.* 28, 3163 (2015).
6. K. Sato and H. Katayama-Yoshida, *J. Appl. Phys.* 40, L485 (2001).
7. S.Y. Wu, H.X. Liu, L. Gu, R.K. Singh, L. Budd, M. van Schilfgaarde, M.R. McCartney, D.J. Smith, and N. Newman, *Appl. Phys. Lett.* 82, 3047 (2003).
8. A.L. Ruoff and T.A. Grzybowski, *Solid State Physics Under Pressure*, ed. S. Minomura (Tokyo: Terra Scientific, 1985), .
9. C. Noguera, *Physics and Chemistry of Oxides Surface* (Cambridge: Cambridge University Press, 1996).
10. I.S. Elfimov, A. Rusydi, S.I. Csiszar, Z. Hu, H.H. Hsieh, H.-J. Lin, C.T. Chen, R. Liang, and G.A. Sawatzky, *Phys. Rev. Lett.* 98, 137202 (2007).
11. V. Pardo and W.E. Pickett, *Phys. Rev. B* 78, 134427 (2008).
12. V.I. Anisimov, J. Zaanen, and O.K. Andersen, *Phys. Rev. B* 44, 943 (1991).
13. V.I. Anisimov, I.V. Solovyev, and M.A. Korotin, *Phys. Rev. B* 48, 16929 (1993).
14. L. Jina and C. Zhou, *Prog. Nat. Sci Mater.* 23, 413 (2013).
15. I. Leonov, V.I. Anisimov, and D. Vollhardt, *Phys. Rev. Lett.* 112, 146401 (2014).
16. B. Doumi, A. Mokaddem, L. Temimi, N. Beldjoudi, M. Elkeurti, F. Dahmane, A. Sayede, A. Tadjer, and M. Ishak-Boushaki, *Eur. Phys. J. B* 88, 93 (2015).
17. B. Doumi, A. Mokaddem, F. Dahmane, A. Sayede, and A. Tadjer, *RSC Adv.* 112, 92328 (2015).
18. S. Berri, A. Kouriche, D. Maouche, F. Zerarga, and M. Attallah, *Mater. Sci. Semicond. Process.* 38, 101 (2015).
19. Z. Wu and R.E. Cohen, *Phys. Rev. B* 73, 235116 (2006).
20. P. Hohenberg and W. Kohn, *Phys. Rev. B* 136, 864 (1964).
21. W. Kohn and L.J. Sham, *Phys. Rev. A* 140, 1133 (1965).
22. P. Blaha, K. Schwarz, G.K.H. Madsen, D. Kvasnicka, and J. Luitz, *WIEN2 K, an Augmented Plane Wave + Local orbitals Program for Calculating Crystal Properties* (Wien: Karlheinz Schwarz, Technische Universität, 2001).
23. H.J. Monkhorst and J.D. Pack, *Phys. Rev. B* 13, 5188 (1976).
24. J.D. Pack and H.J. Monkhorst, *Phys. Rev. B* 16, 1748 (1977).
25. P. Reunchan, N. Umezawa, S. Ouyang, and J. Ye, *Phys. Chem. Chem. Phys.* 14, 1876 (2012).
26. Y. Liu, W. Zhou, and P. Wu, *J. Appl. Phys.* 121, 075102 (2017).
27. J. Bai, J.-M. Raulot, Y. Zhang, C. Esling, X. Zhao, and L. Zuo, *Appl. Phys. Lett.* 98, 164103 (2011).
28. B. Doumi, A. Mokaddem, M. Ishak-Boushaki, and D. Bensaid, *Sci. Semicond. Process.* 32, 166 (2015).
29. F.D. Muranghan, *Proc. Natl. Acad. Sci. USA* 30, 244 (1944).
30. Y. Sato and R. Jeanloz, *Geophys. Res.* 86, 11773 (1981).
31. L.-G. Liu and W.A. Bassett, *J. Geophys. Res.* 78, 8470 (1973).
32. K.L. Yao, G.Y. Gao, Z.L. Liu, and L. Zhu, *Solid State Commun.* 133, 301 (2005).
33. G.Y. Gao, K.L. Yao, E. Şaşıoğlu, L.M. Sandratskii, Z.L. Liu, and J.L. Jiang, *Phys. Rev. B* 75, 174442 (2007).
34. M. Labidi, S. Labidi, S. Ghemid, H. Meradji, and F. El Haj Hassan, *Phys. Scr.* 82, 045605 (2010).
35. R.J. Zollweg, *Phys. Rev.* 111, 113 (1958).
36. J.P. Perdew, K. Burke, and M. Ernzerhof, *Phys. Rev. Lett.* 77, 3865 (1996).
37. K. Sato, P.H. Dederichs, K. Araki, and H. Katayama-Yoshida, *Phys. Status Solidi C* 7, 2855 (2003).
38. H. Akai, *Phys. Rev. Lett.* 81, 3002 (1998).